Proceedings of the 41st Turbomachinery Symposium
September 24-27, 2012, Houston, Texas

Comparison of different variable speed compression train configurations with respect to rotordynamic stability and torsional integrity

Reto Somaini
Mechanical development
MAN Diesel & Turbo Schweiz AG
Zürich, Switzerland

Mr. Somaini graduated as Mechanical Engineering in 2006 at the ETH (Swiss Federal Institute of Technology) in Zurich. Since then he's active for MAN Diesel & Turbo Schweiz AG, with a major focus on the care of magnetic bearing machines from 2007 onwards. The job tasks include rotordynamic support and analysis for the commissioned projects and technical bid support for the high speed compressors.

Yves Bidaut
Manager Mechanical Development
MAN Diesel & Turbo Schweiz AG
Zürich, Switzerland

Yves Bidaut is manager of the mechanical development department of MAN Diesel & Turbo Schweiz AG in Zürich, Switzerland. His job function includes the development and analysis of the components of centrifugal compressors for the Oil & Gas application. He is responsible for providing technical support in rotordynamics and stress analysis. Before joining the site in Switzerland in 2003 he was employed for 6 years in MAN Diesel & Turbo, Berlin where he was involved in the design, finite element analysis, rotordynamic analysis, testing and development of centrifugal compressors.
He received his diploma (Mechanical Engineering, 1995) from the University of Valenciennes (France).

Baumann Urs
Head of Calculation and Development
MAN Diesel & Turbo Schweiz AG
Zürich, Switzerland

Urs Baumann is the Head of the Calculation and Development department of MAN Diesel & Turbo Schweiz AG, in Zurich, Switzerland. His responsibilities include the aerodynamic and mechanical improvement of turbocompressors and associated components, as well as the implementation and maintenance of test stands and analytical tools needed to perform this task.
Before joining MAN Diesel & Turbo in 1996, Mr. Baumann worked for Sulzer Innotec, the Corporate Research and Development Center of Sulzer Ltd. For several years he was in charge of the machinery dynamics group that is responsible for the development, design improvement and troubleshooting on a wide range of Sulzer products.
Mr. Baumann has a diploma (Mechanical Engineering, 1987) from the Swiss Federal Institute of Technology in Zurich.

ABSTRACT

Wherever a variable speed gas compression train is needed for Oil & Gas upstream applications as well as for gas storage applications the primary decision has to be made between a gas turbine driver and an electric motor controlled by a variable frequency drive (VFD). A second decision has to be made between a high speed direct driven train and a low speed driver (gas turbine or motor) driving the compressor via a speed increasing gear. Finally it has to be decided whether a classical, oil lubricated train arrangement shall be used or if a high speed, oil-free, magnetic bearing levitated train configuration shall be chosen. With these three major decisions a variety of different train configurations are possible. They differ from each other in many technical aspects and therefore have strengths and weaknesses which can be rated in order to facilitate the evaluation of the optimum equipment configuration for a certain application.

This paper specifically concentrates on the comparison of rotordynamic key figures like the logarithmic decrement (damping) of the lowest bending mode, the presence of overhung coupling modes within the speed range or the presence of torsional critical speeds which can be excited within the speed range and which therefore might adversely affect the integrity of the train components. The evaluated configurations include modern hermetically sealed, oil-free, magnetic bearing levitated compressor designs. Based on these key figures this paper will benchmark the rotordynamic

robustness as well as the operational safety of the investigated train configurations.

INTRODUCTION

In the past, the driver of choice for Oil & Gas upstream and midstream applications was the gas turbine. Especially when speed variation was necessary to meet the process requirements for a wide operating range and a large turn down. Gas turbine driven compressor trains can either be directly driven (high speed gas turbine without gearbox) or can consist of a low speed gas turbine driving the compressor via a speed increasing gearbox. Environmental restrictions like local pollution regulations and noise requirements as well as the complexity of the gas turbine system (infrastructure and certainly also maintenance aspects) have led to a steadily increased demand for electric (VFD) driven compressor trains. Concurrently also the variable frequency drives (VFD's) for electric motors have evolved greatly with respect to available powers and reachable frequencies. Finally, in the last ten years a completely new type of compressor for these applications has entered the market, the so called sealed, oil-free, compact compression systems, levitated by active magnetic bearings (AMB) and driven by high speed motors.

These different compression systems all have their strengths and also their shortcomings. Gas turbine systems are surely preferred when gas is readily available whereas motor driven systems have their advantages on the availability and maintenance side. Finally, sealed, compact compression systems are best suited for environmentally critical applications due to their zero leakage design or for applications where space and weight is key. Beside these economic and operational differences the described systems differ also greatly with respect to rotordynamic aspects.

This paper addresses the most important and safety relevant rotordynamic criteria:

- Logarithmic decrement (damping) of the lowest whirling mode (a measure for the basic, inherent stability of the arrangement) and the maximum tolerable cross coupling train loading.
- The presence of critically damped modes near or within the speed range (allowed by API 617 due to their low amplification factor, but nevertheless introducing and adverse unbalance sensitivity). Those are normally overhung coupling modes for the compressors on oil bearing and mostly rigid body modes in those on magnetic bearings.
- The presence of torsional critical speeds which can be excited within the speed range and which might therefore adversely affect the integrity of the train components.

This paper will judge and rank the different systems with respect to these criteria in order to facilitate the evaluation of the optimum equipment configuration for a certain application.

DESCRIPTION OF THE INVESTIGATED SYSTEMS

General Arrangements

In this chapter the five investigated train configurations and their design specific rotordynamic aspects are described and explained.

Configuration 'A'

In configuration 'A' the compressor is driven via a flexible coupling. The gearbox increases the speed from the turbine shaft at 9048 to 11270 rpm for the compressor and thus has a gear ratio of ~1.25. When the gear ratio is less than two and the train has to run in a large speed spectrum, the low and high speed ranges merge in on single extremely large prohibitive region. It becomes almost impossible to shift the torsional frequencies out by tuning the coupling stiffness.

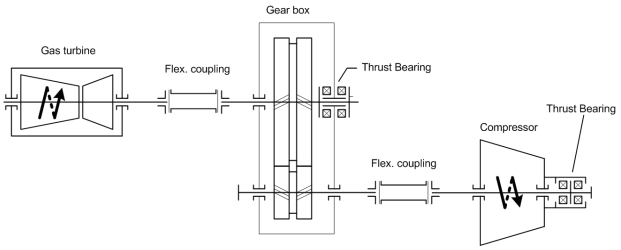

Figure 1. Configuration A, Low Speed Gas Turbine Driving the Compressor Via a Speed Increasing Gearbox.

In terms of lateral bending characteristic the machine does not have any specialties.

Configuration 'B'

A VFD with 50 Hz line frequency feeds the 1800 rpm synchronous motor. The motor drives the compressor via gearbox and two flexible couplings.

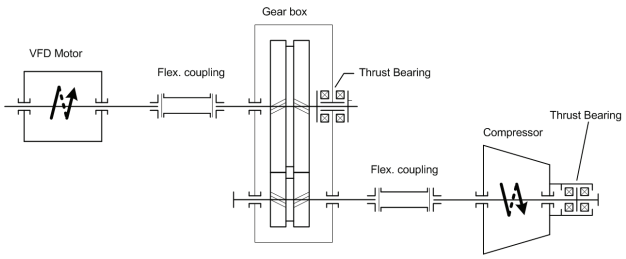

Figure 2. Configuration B, Low Speed Electric Motor Driving the Compressor Via a Speed Increasing Gearbox.

The torque ratings of flexible couplings for motor driven compressors are substantially higher because they have to cope with the occurring air gap torques. Therefore, for high power and torque applications a lateral drive end overhung critical speed is expected in or near the operating speed range causing increased coupling unbalance sensitivity (an on site trim balancing of the coupling might be necessary). The gearbox brings the speed from 1797 to 11277 rpm.

Configuration 'C'

With respect to the compressor lateral critical speeds this configuration is identical to configuration 'A'. The torsional analysis of this arrangement is usually uncritical due to the non-existing torque excitations of the gas turbine drive and the fact that the first torsional eigenfrequency can be tuned below

minimum speed (soft coupling) while the second clearly remains above the speed range. Since there is no speed increasing gearbox necessary in this configuration even the possible excitations from this source cannot occur. The operation speed range extends from 5638 to 11840 rpm.

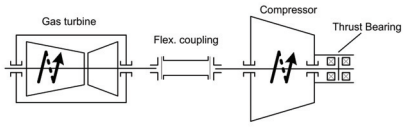

Figure 3. Configuration C, High Speed Gas Turbine, Direct Compressor Drive

Configuration 'D'

Configuration 'D' is one representative for the new generation of high speed motor driven, magnetically levitated compact compression systems. Even though the schematics for the configurations 'C' and 'D' shown in Figures 3 and 4 look very similar the real systems are completely different. In this configuration each train component - motor and compressor - come with their own pair of radial bearings (as opposed to the following configuration 'E') and the axial bearing is moved from the overhang position to the new location between the radial bearings.

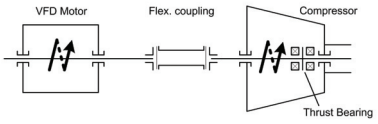

Figure 4. Configuration D, High Speed Electric Motor, Direct Compressor Drive Via a Flexible Coupling

Since the compressor is driven via a flexible coupling the issue of the drive end coupling overhung mode is also present for this configuration.

The key of this configuration is the ability to damp the first bending mode critically allowing the operation of this train in the full speed range of 30-105 percent which is 3375 to 11813 rpm.

With regard to the torsional analysis all the issues of VFD driven trains do also apply here.

Configuration 'E'

Configuration 'E' is a second representative of the new generation of high speed motor driven, oil-free, hermetically sealed compressors. Here the motor and the compressor shafts are connected to each other by a rigid coupling, thus resulting in one single shaft component, see Figure 5.

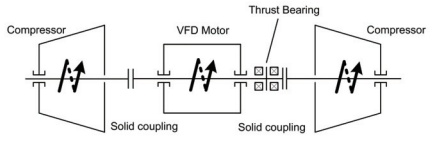

Figure 5. Configuration E, High Speed Electric Motor, Direct Compressor Drive, Entire Arrangement on One Solid Shaft.

As the compressor is driven by frequency converter non-integer harmonics can occur also for this configuration.

Thermodynamic Layout

The duty of a gas storage compressor station requires an extremely large bandwidth of volume flow over the whole pressure field between the pipeline pressure and the maximum allowed storage pressure. To optimize the use of storage stations a withdrawal of stored gas down to the minimum cavern pressure is more and more planned resulting in an extremely wide operational map for the compressor station. To meet all the design point requirements, the compressor is designed as intercooled two sections machine, with the possibility of serial and parallel operation modes of the sections. All five presented configurations are able to run in series and in parallel.

The train has to deliver 1.0 m3/s natural gas (mole weight ca 16.5 kg/kmol) up to 206 bar in serial operation and consumes 7 MW. In parallel operation the train shall deliver nearly double flow. The impeller tip diameter is around 400 mm.

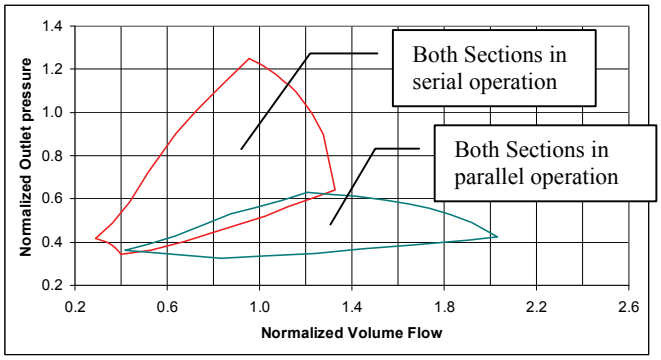

Figure 6. Compressor Performance Map (Conf. 'E').

The thermodynamic layout of each single machines is chosen as such, that a similar performance map is common to all trains (example of configuration 'E' shown in Figure 6). The thermodynamic duty is taken from a real storage project as the configurations shall represent a real scenario.

Train configurations 'A', 'B' and 'C' have a conventional intercooled barrel compressor design with eight stages. The first sealed magnetically levitated configuration presented ('D') is still an inline intercooled barrel compressor, but the impeller design is slightly different, because the first impellers of each section have to provide the cooling gas for the motor and for the magnetic bearing respectively. The cooling gas flow needed can be a substantial part of the overall mass volume flow. These considerations are valid also for configuration 'E' but there the compressor has a different impeller layout (see description in the following chapter).

The table below shows an overview of the operating speed ranges of the different trains.

Configuration	Low speed shaft min.-max. speed	High speed shaft min.-max. speed	Speed Range (%)
'A'	4524 - 9500	5635 - 11833	50-105
'B'	899 - 1887	5642 - 11843	50-105
'C'	-	5638 - 11840	50-105
'D'	-	3375 - 11813	30-105
'E'	-	3429 - 12000	30-105

Table 1. Low and high speed shaft operating ranges in rpm

Main characteristics of the compressors

Compressors of Configurations 'A', 'B' and 'C'
For the three conventional arrangements the thermodynamic layout, the dry gas seals as well as the radial and the axial bearings are exactly the same. Only the driven shaft ends and the weights / inertias of the couplings are different due to maximum peak torque of the different driver types.
As an example of this category the compressor 'C' is shown in Figure 7, with the coupling installed on the left side.

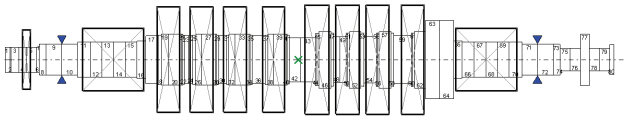

Figure 7. Compressor model of configuration 'C'.

On the non driven end the axial bearing is placed in overhung design to reduce bearing span and for easy access.

Compressor of Configuration 'D'
Thanks to the hermetically sealed design there is no need for dry gas seals. The magnetic thrust bearing is placed inboard and is designed to deliver thrust forces needed for the safe operation in the whole performance map without the help of a controlled pneumatic system.

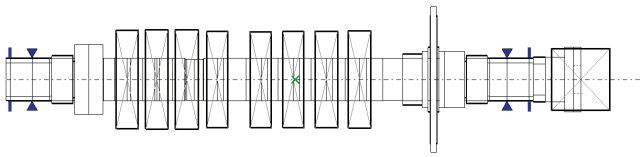

Figure 8. Compressor model of configuration 'D'.

In the Figure 8 the coupling hub is already modeled (on the right side), and only the spacer weight is placed as concentrated mass.

Compressor of Configuration 'E'
As this configuration has the ability to carry more impellers, a compressor design with 10 stages of smaller diameter is chosen. The aim is to operate with a better efficiency. The compressor is split in a 5 stage low pressure part on the left of the motor and a 5 stage high pressure part on the opposite side.

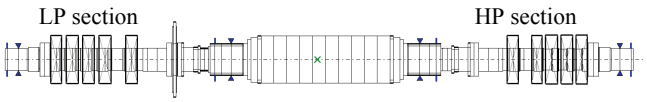

Figure 9. Shaft model of configuration 'E'

The axial bearing is placed between motor and low pressure compressor.

Due to this rather unusual design (compared to the other investigated configurations) the lateral as well as the torsional analysis results look very much different. There is obviously no coupling overhung mode, the mode shapes of the lateral critical speeds look different to conventional ones and finally also the torsional criticals are different because this system is torsionally very stiff. Of course, all the issues of the VFD's excitations have to be addressed also in this configuration.

LATERAL ANALYSIS – GENERAL CONSIDERATIONS

In order to estimate the differences (and analogies) between the different configurations regarding their lateral behavior an overview of some general characteristics (critical speed map, bearing characteristics) is shown in the following paragraphs.

Undamped Eigenvalue Analysis

The critical speed maps (showing the frequencies of the undamped critical speeds in dependence of the support stiffness) are shown in Figure 10 (for the three oil-bearing configurations) and Figure 11 for both active magnetic bearing configurations. Instead of the bearing stiffness path, the critical speeds resulting from the response analysis presented afterwards are superimposed on the speed map.

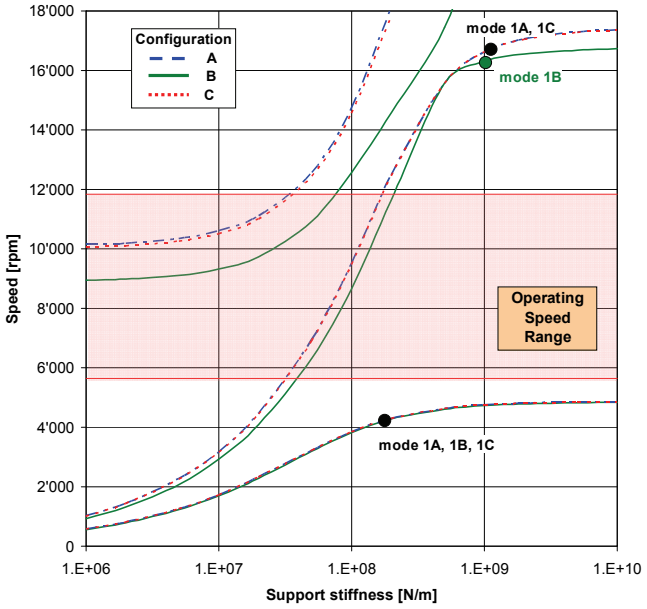

Figure 10. Combined Speed map for all oil bearings configurations.

It can clearly be seen that all the three configurations 'A', 'B' and 'C' run free of any critical speed. Furthermore the comparison reveals that they are comparable regarding the first bending and the conical mode. Only at the frequency of the coupling overhang mode for 'B' is significantly lower than for the similar configurations 'A' and 'C'. This is the direct consequence of the heavier coupling due to the motor driver instead of the gas turbine driver for 'A' and 'C'. Although this mode is outside the operating speed range the sensitivity to any coupling unbalance for all configurations will be investigated in more depth further on.
The lateral critical speed map for the rotor 'D' shows similar behavior as for the three conventional previous configurations. Because of the larger bearing span (due to the axial bearing that is installed between both journal bearings) the critical speeds are shifted towards lower values. Together with an assumed value of the effective bearing stiffness of 5e7 N/m two critical

speeds are now expected to be within the operating speed range and must therefore be critically damped. As explained by Kleynhans, et al. (2005) the critical speed behavior for compressors designs analogous to configuration 'E' is completely different to the four previous discussed. The four journal bearings (they reduce the bearing span) and the solid couplings make the rotor much stiffer. This is visible on the right side of the speed map in Figure 11. Nevertheless resonances occur at four frequencies corresponding to the modes 1E, 2E, 3E and 4E.

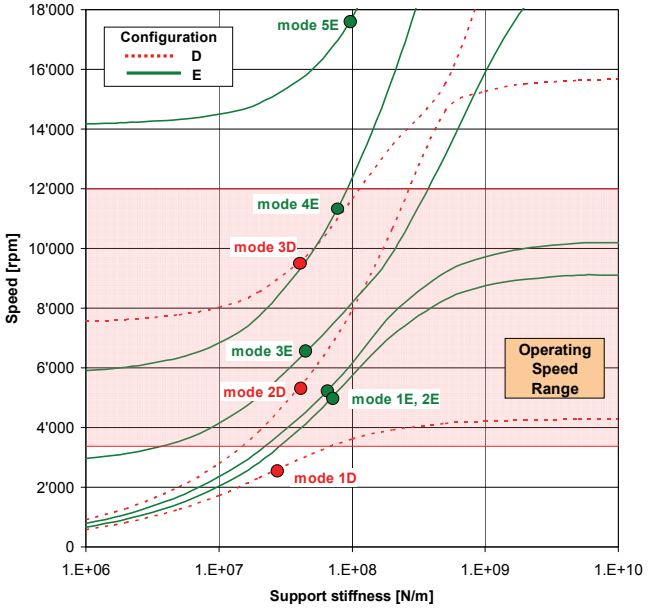

Figure 11. Combined Speed map of both magnetically levitated configurations.

The associated mode shapes at an expected effective bearing stiffness of 5e7 N/m are represented in Figure 12. From the speed map of magnetically levitated compressors it is visible that there are lateral bending modes in the operational speed range. Those modes must be critically damped according to the API 617 (2002) requirements in §2.3.6.

The mode shapes of configuration 'D' as shown in Figure 12 are similar to the conventional ones. Because of the four bearing suspended rotor the mode shapes for configuration 'E' are a unusual and the naming of the modes becomes difficult. The first mode (denominated as 1E) is a parallel mode; the second mode 2E is a tilting mode over the whole assembled rotor (compressor – motor – compressor). The shapes are not "pure" since they are influenced by the ratios of translational mass inertia to the bearing force / stiffness. The third mode (3E) is a kind of overall bending mode whereas the fourth (4E) is a Z-mode (or overall conical) but with still straight single rotors. The first mode with a real accentuated bending in the compressors is above maximum continuous speed. This last consideration is valid for the first mode above the speed range of configuration 'D' too. Therefore a sufficient separation margin is required to avoid increased vibration at maximum operating speed.

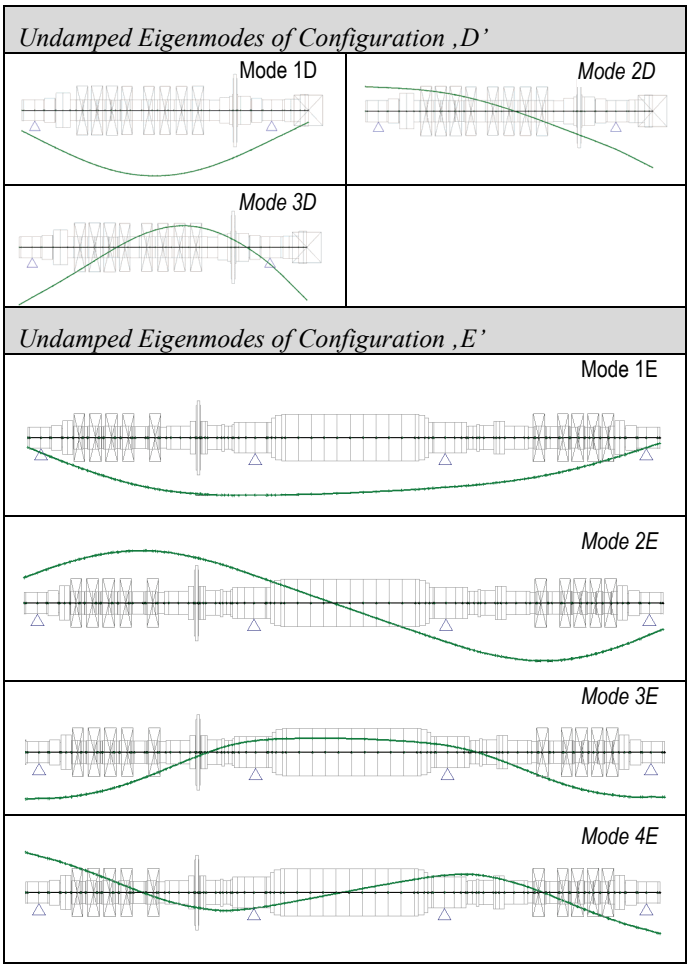

Figure 12. Undamped critical Speed Mode Shapes.

Bearing Characteristics

The design of the oil bearing is a robust four tilting pad bearing (TPB in short notation) with load between pads and a light pivot offset of 0.56. The magnetic bearings of configurations 'D' as well as the NDE compressor bearings of configuration 'E' are chosen identical in diameter and length, whereas the motor bearings in configuration 'E' are bigger and have therefore higher capacity.

In order to perform a proper comparison between the different configurations identical oil-lubricated journal bearings are used for all 'conventional' compressors ('A', 'B' and 'C') and a typical transfer function is used for the two magnetic bearing configurations (not using any special control features to increase the damping).

The synchronous filters do not provide improvements on the train stability. Those filters can lower the amplification factor for synchronously excited modes, e.g. unbalance. But as soon as subsynchronous excitations arise, the mode has its original damping characteristic.

In Figure 13 the common transfer function is shown. In configuration 'E' the gain of the transfer function of the bigger motor bearings has been scaled with the bearing capacity. Indeed there is potential to optimize the single solutions for 'D' and 'E' with an own specialized transfer function, but the

comparison of modal analysis results would be less representative. The oil bearing damping and stiffness are plotted in the gain / phase format usual for AMB transfer functions.

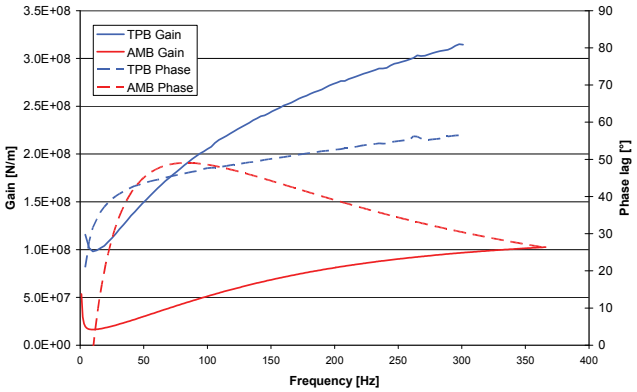

Figure 13. AMB transfer function and TPB characteristic.

Although Figure 13 gives a good visual comparison, for stability considerations the characteristics at the actual running speed (synchronous) have to be taken for the oil bearing machines, whereas for the configurations with magnetic bearings the gain and phase are taken at the excitation frequency (asynchronous).

The gain of oil bearing is bigger by a factor of five at low frequency and of three at maximum continuous speed (around 200 Hz). The second important note is the negative AMB phase at low frequency which gives a negative damping coefficient. Thus the system of shaft and bearings has to be designed in a way that no mode appears below approximately 10 Hz.

LATERAL ANALYSIS - EVALUATION

Harmonic Response Analysis

A harmonic response analysis is carried out for all the configurations. The calculation is based on the bearing characteristics presented in Figure 13.
The calculation results tabulated in Table 2 show that all the trains fulfill the criteria for the separation margins according to API 617 (2002) §2.6.2.10. The table shows also the required separation margin SMreq. for the associated amplification factor.
All conventional configurations run between the first bending mode at 4420 rpm and the 1st conical mode located at 16300-16700 rpm depending upon the compressor drive end overhang dimensions. In representation of the three oil bearing machines the exemplary unbalance response of configuration ‘A’ is shown in Figure 14.
Due to the heavier drive end overhang design configuration ‘B’ has the higher amplification factor on the conical mode as the gas turbine driven layouts.
When the bearing characteristics are soft, rigid body modes easily occur at relatively low speed even if the rotor exhibits enough bending stiffness. For configuration ‘D’ this is the case leading to a really high flexi-ratio (maximum continuous speed divided by lowest lateral modal frequency). Regarding the unbalance response analysis the shaft stiffness combined with soft bearings helps the magnetic bearing controller to damp the mode to a low amplification factor and often the API 617 §2.6.2.10 criteria are fulfilled for rigid body modes.

Mode	Speed	AF	$SM_{req.}$	$SM_{effect.}$
	[rpm]	[-]	[%]	[%]
Configuration ‘A’				
1st bending	4420	4.5	11.3	21.6
1st conical	16650	3.6	18.7	40.6
Configuration ‘B’				
1st bending	4420	4.6	11.5	21.6
1st conical	16350	7.3	24.1	38.1
Configuration ‘C’				
1st bending	4420	4.5	11.3	21.6
1st conical	16650	3.6	18.7	40.6
Configuration ‘D’				
1st parallel	2761	1.4	None	18.2
1st tilting	5278	0.9	None	w.s.r.
1st bending	9574	1.3	None	w.s.r.
Configuration ‘E’				
1st parallel	5499	0.9	None	w.s.r.
1st tilting	5544	1.1	None	w.s.r.
1st bending	6324	2.0	None	w.s.r.
Z-mode	11621	2.0	None	w.s.r.
1st bending compressors	17756	4.8	21.8	48.0

Table 2. Critical Speed Analysis (w.s.r.: within speed range).

Indeed there are, for configuration ‘D’, some more critically damped modes within the speed range, resulting in a combination of bending and overhung deflected modes.

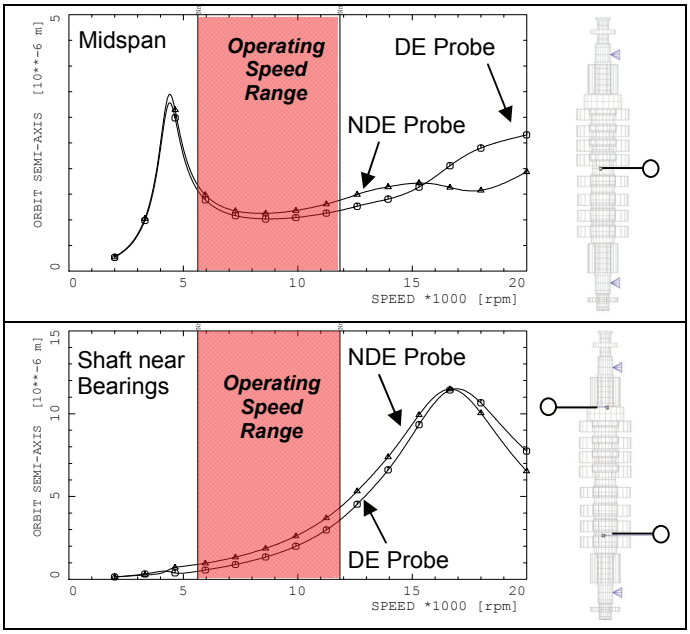

Figure 14. Harmonic Response of Configuration ‘A’.

For configuration ‘E’ the thoughts presented for ‘D’ can be transferred only partially. Due to shorter bearing spans and rigid couplings the parallel mode is located in the lower part of the speed range (at 5499 rpm) and is considerably higher than in all others configurations. This mode is extremely near to the tilting mode at 5555 rpm. In the end, configuration ‘E’ has the

greatest number of critically damped modes within the speed range. This can lead to phase changes which - together with the 4 bearings arrangement - make the balancing of the rotor more challenging in comparison to the other configurations.
The following ranking summarizes the presented considerations:

1. Configuration ‘A’ & Configuration ‘C’
2. Configuration ‘B’
3. Configuration ‘D’
4. Configuration ‘E’

Coupling Overhung Mode

Especially at higher powers and torques couplings are heavy and therefore lower the drive end side overhung mode into the operating speed range. Even though these overhung modes are usually well (critically, according to API 617) damped, they result in an increased coupling unbalance sensitivity which, in many cases, makes it necessary to trim balance the coupling on site. Normally such high vibrations can be successfully reduced by a trim balancing of the coupling. On the other hand the coupling as the joining element is the most critical in terms of on site assembly and repeatability.

The unbalance sensitivity is mainly influenced by the amplification factor. To ensure a fair comparison between the different configurations a standard reversed hub coupling (same design but with the necessary rating for the appropriate configuration) is used. According to the design of configuration ‘E’ no flexible coupling is needed. Nevertheless the coupling unbalance sensitivity is determined in the same way.

The placed unbalance amount is calculated as follows:

$$U_{Cpl} = 6350 \cdot \frac{M_{CH}}{N_{mcs}} \cdot 10 \qquad (1)$$

U_{Cpl}: Coupling Unbalance [gmm]
M_{CH}: Mass of Coupling Half [kg]
N_{mcs}: max. continuous Speed [rpm]

This unbalance corresponds to 10x API unbalance - a balance quality of 6.65 - which is equal to the maximum unbalance allowed after dismantling and reassembling the coupling when balanced according to API 671 (2007) §2.6.3.6.

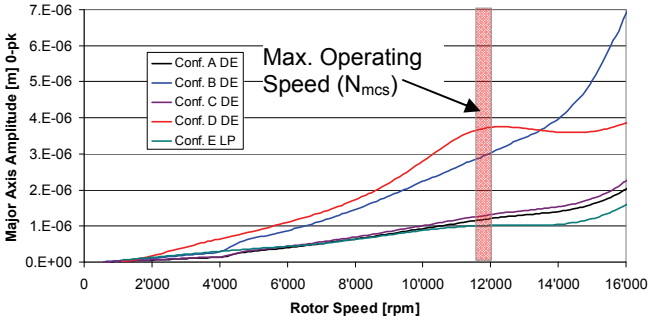

Figure 15. Coupling sensitivity for the different configurations

Figure 15 shows the vibration level for the coupling unbalance case over the speed. The resulting amplitude at maximum operating speed is divided by the set unbalance to extract the influence coefficient of the coupling unbalance. More detailed information is delivered by Table 3 where the half coupling mass, the unbalance set, the resulting vibration amplitude and the influence coefficient is shown. For a better comparison the coupling weight of configuration ‘E’ includes the axial disk weight because the disk is located between LP compressor flange and motor thrust end coupling hub.

Configuration:	‘A’	‘B’	‘C’	‘D’	‘E’
½ Cpl. Mass [kg] M_{CH}	19.6	39.2	21.2	26.4	*31.7*
Unbalance [gmm] U_{Cpl}	105.3	210.0	113.6	141.6	167.7
Max. Amplitude 0-pk [µm] at N_{mcs}	1.2	3.0	1.3	3.8	1.0
Influence coefficient [µm/kgmm]	11	14	12	27	6

Table 3. Coupling Sensitivity.

Configuration ‘B’ clearly has higher sensitivity (heavier coupling, mode nearer to Nmcs) as the configurations ‘A’ and ‘C’. The solution ‘D’ has the disadvantage of softer bearings and it is visible that a mode is present beyond the Nmcs of 11813 rpm. This automatically results in a higher vibration and thus coupling sensitivity. Train ‘E’ has the convenience that the coupling is not really located at overhang but at midspan, greatly reducing the vulnerability for coupling unbalances. Configuration ‘D’ and ‘B’ have a similar coupling because of the motor driver.
Thus the ranking regarding coupling sensitivity is:

1. Configuration ‘E’
2. Configuration ‘A’
3. Configuration ‘C’
4. Configuration ‘B’
5. Configuration ‘D’

Since the coupling in configuration ‘E’ is a solid flange connection, it is very unlikely that the unbalance state will increase by a factor of 10 just by disconnecting the flange.

API 617 Level I Stability Analysis

Since no gas forces (rotor-stator interaction forces) are considered the calculation of the basic (unloaded) logarithmic decrement (LogDec) of the lowest bending mode of a rotor is not sufficient for the assessment about the stability of the compressor in operation but it provides an indication for the inherent stability of a compressor design. The basic LogDec (δ_b) is mainly a function of the rotor stiffness or flexibility represented by the flexi-ratio (defined as the maximum continuous speed divided by the frequency of the lowest bending mode) in combination with the ability of the bearing to introduce damping into the rotor.

For the calculation of the stability the bearing characteristics described in the general consideration to lateral analysis shown in Figure 13 are used.

The conventional compressors in configurations ‘A’ to ‘C’ show a basic logarithmic decrement of 37-38 percent, while both the magnetic bearing machines achieve a higher δ_b. Due to its large deflection at the bearing locations the compressor of configuration ‘D’ delivers larger damping than configuration ‘E’ (δ_b is 549 percent and 192 percent respectively).

In order to estimate the stability behavior of the compressors at operating (loaded) conditions and to compare them between each other a Level I analysis is carried out according to API 617 (2002). The anticipated cross coupling Q_A= 4.22 kN/mm is applied for each configuration.

The results shown in Figure 19 indicate that all the configurations are stable in loaded conditions (δ_A> 10 percent).

To determine the sensitivity of the compressor to destabilizing effects the magnitude of the cross-coupling stiffness is varied. The applied cross coupling stiffness is extended from 0 (unloaded) to the amount required to produce a zero LogDec (Q_0).

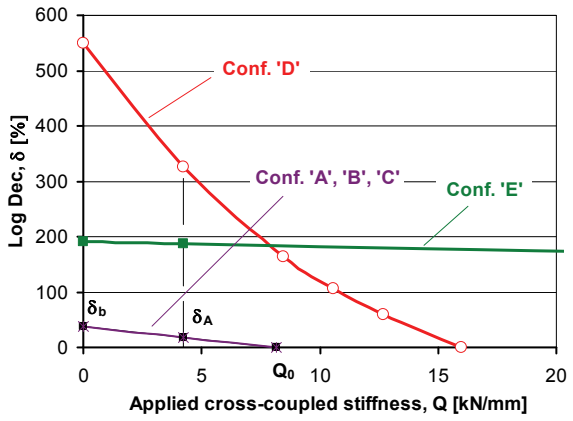

Figure 16. Stability Diagram

Figure 16 indicates that both magnetic bearing configurations provide a much higher LogDec at the anticipated cross coupling (δ_A) than the conventional configurations. But even though configuration 'D' yields the highest δ_A by far, it also shows a very steep drop on the LogDec as a function of the cross coupling resulting in surprisingly low Q_0.
Configuration 'E' does not show the same behavior as configuration 'D' because the flexi-ratio is lower and the aerodynamic forces are distributed over four bearings and not only two. In addition as the motor bearings have a larger size they can provide more net damping forces. The discussed results of the Level I analysis are summarized in Table 4.
For the conventional configurations a Q_0 of around 8 kN/mm is determined, whereas a Q_0 of 16 kN/mm is calculated for configuration 'D'. The same calculation done for configuration 'E' leads to a Q_0 of 80 kN/mm.

Configuration	'A'	'B'	'C'	'D'	'E'
Basic LogDec δ_b [%]	38	37	38	549	192
LogDec δ_A [%] (Q_A applied)	18	18	18	326	188
Cross Coupling Q_0 [MN/m]	8.2	8.0	8.2	16	80
Ratio Q_0/Q_A	1.9	1.9	1.9	3.8	19.0
Critical Speed Ratio CSR [-]	2.4	2.5	2.4	2.8	1.3
Level I Stability Analysis					
i) $Q_0/Q_A < 2$	*yes*	*yes*	*yes*	*no*	*no*
ii) $\delta_A < 0.1$	*no*	*no*	*no*	*no*	*no*
iii) $2.0 \leq Q_0/Q_A < 10$	*no*	*no*	*no*	*yes*	*no*
CSR in region	*B*	*B*	*B*	*B*	*A*
Level I fulfilled ?	No	No	No	No	Yes

Table 4. Summary of Level I Analysis

As the average gas density is around 55 kg/m3, the Level I Criteria are fulfilled only by the magnetic bearing levitated machine of configuration 'E'. A non-compliance on the level I criteria does not indicate a dangerous condition for the system in terms of stability. It states only that a closer look has to be given at the labyrinth seals and that the compressor manufacturer has to ensure enough damper devices (such as swirl brakes or shunt holes) are present in the machine's design.
The comparison of Q_0 between all configurations leads to the conclusion that the four magnetic bearings configuration 'E' is superior to the others by far. Configuration 'D' has promising basic LogDec δ_b and Q_0 but the decay of LogDec is steep and therefore difficult to correct with damping devices. A prediction of the stability in the field is strongly dependent of the effective labyrinth stiffness and damping coefficients and modal damping will most probably drop when the machine is loaded. Configuration 'A' to 'C' have first to compensate their relatively low basic LogDec and need a stabilizing effect of the seals when the machine is loaded to reach similar loaded LogDec as the two magnetic bearing configurations. The stabilizing effect can be achieved with less effort than in configuration 'D'.
Regarding stability the four magnetic bearing arrangement 'E' outclass the oil bearing configurations. Configuration 'D' has a very high δ_b but a strong decay over cross coupling.

Parametric Damping Study for AMB equipped configurations

For both magnetically levitated configurations 'D' and 'E' modes are within the operating speed range. According API 617 (2002) §2.6.2.10 the amplification factor for these modes (mode 2D/3D and modes 1E…4E) has to be below 2.5, calling for a modal damping greater than 20 percent. This leads to requirements towards the magnetic bearing supplier to come up with an appropriate transfer function. Even if many interesting advantages can be obtained with the greater degree of freedom with magnetically levitated systems not every arbitrary poor shaft design can be well damped.
A modal analysis of the system brings insight in the damping behavior regarding critically damped modes and stability.
A plot of modal damping as a function of calculated natural frequencies (root locus plot) is presented in Figure 17. The plot includes results for all relevant (forward) modes of the compressor model, with calculated natural frequencies below 350 Hz. Each line represents a separate mode and is composed of data points that encompass a bearing damping range of 0 kNs/m (no damping at bearing) to 120 kNs/m (very large damping). According to the API 617 specifications (regarding Separation Margin and Amplification Factor) a prohibited range labeled "API Safety zone" is superimposed in the diagrams.

For the configuration 'D' the results indicate that two modes (Mode 2D and Mode 3D) require sufficient damping to be provided by the AMB in order to fulfill the API-specification. Furthermore the figure illustrates that not all modes can be damped in the same manner: while all other modes reach top modal damping, mode 4D remains below 15 percent for any bearing damping. This is the direct consequence of the low deflection at the bearing locations. However as long as such modes have enough separation margin they do not play a role in the judgments and safety considerations.

What strikes the eye in the second graph of Figure 17 is that configuration ‘E’ presents two additionally critical modes which require a large damping by the AMB (Mode 1E and Mode 4E). This is due to the train arrangement with solid coupling.

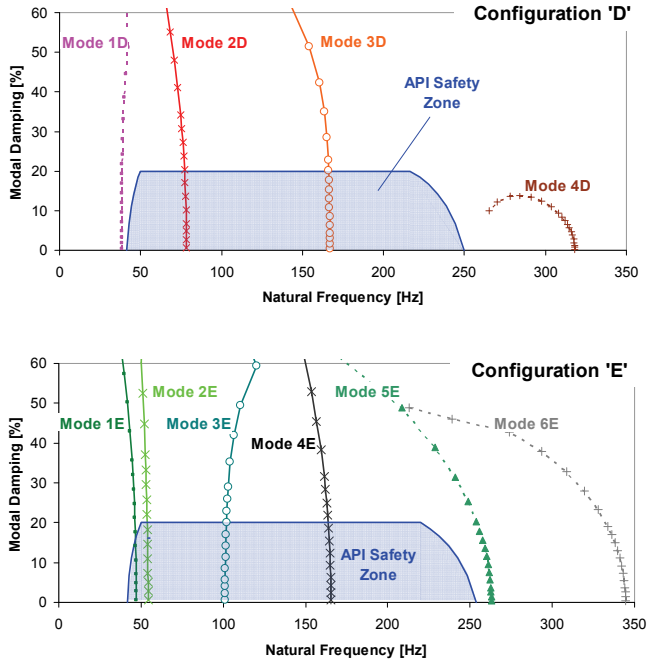

Figure 17. Root Locus Plots

The analysis of system’s modal damping behavior over the parameterized bearing damping is helpful to gain understanding and a qualitative key figure to describe the ability to damp the modes the machine runs on. The influence of the bearing damping on the overall modal damping is shown in Figure 17 for configurations ‘D’ (above) and ‘E’ (below).
During the calculation the bearing stiffness is held constant while bearing damping is varied. Actually there is a dependence on the assumed bearing stiffness leading to different frequencies and different modal damping. Normally stiffer bearings imply a higher natural frequency and a flatter modal damping evolution. A comparison of the behavior of all modes at several bearing stiffnesses would give the outright picture. For the sake of simplicity and overview the damping variation is calculated with typical stiffness for the mode frequency and the stiffness is varied in a second step. For the modes 1D & 1E/2E (natural frequency 30-60 Hz) a constant bearing stiffness of 2e7 N/m is assumed. For higher natural frequencies (75-125 Hz, corresponding to modes 2D&3E) the calculations are performed with a bearing stiffness of 3.5e7 N/m. A bearing stiffness of 5.0e7 N/m is assumed for all the other modes (3D, 4E & 5E), whose natural frequency is greater than 150 Hz. As the comparable modes are investigated at the same bearing stiffness a direct comparison is possible nevertheless.

Figure 18 presents the same eigenmodes as Figure 17. It describes how the modal damping evolves over the variation of bearing damping. The dashed horizontal line in the diagrams represents the required minimum damping of 20 percent (corresponding to AF= 2.5). The intersection of this horizontal line with the modes curves gives the minimum required damping coefficient to be provided by the AMB (called $D_{20\%}$). A low value of $D_{20\%}$ means that the system is easier to handle for the controller. Several modes requiring high damping coefficients – besides limitations from the bearing and the control cabinet – enforce compromises on the overall loop performance.

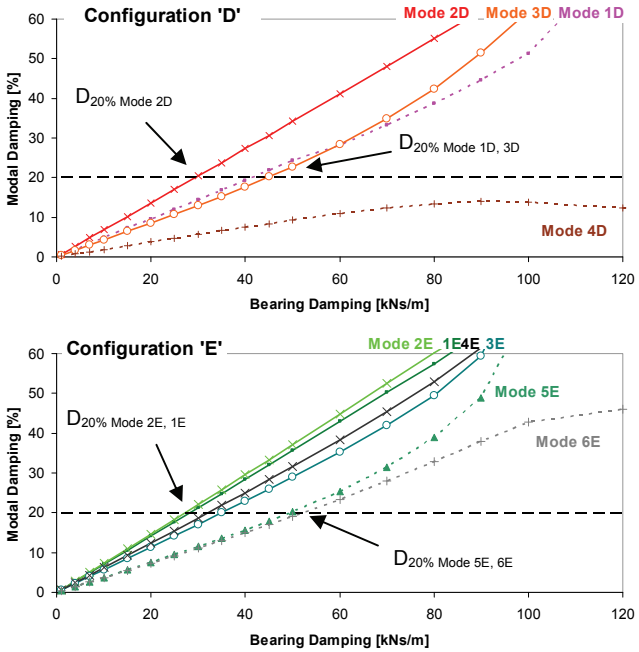

Figure 18. Modal Damping vs. Bearing Damping

From the diagrams it can be derived that mode 2D requires a bearing damping of 29 kNs/m, whereas mode 3D requires 45 kNs/m. For configuration ‘E’ a bearing damping of only 35 kNs/m is required to achieve a modal damping of 20 percent for all the four critical modes.

Table 5 lists the modal damping $D_{20\%}$ and the frequency $NF_{20\%}$ (where a mode reaches $D_{20\%}$) and gives an overview if the modes are in speed range when the specified stiffness is used.

Mode	C_{BRG} [N/m]	$D_{20\%}$ [kNs/m]	$NF_{20\%}$ [Hz]	Within sp.range?
Mode 1D	2.0e7	41.4	36	*no*
Mode 2D	3.5e7	29.4	77	*YES*
Mode 3D	5.0e7	44.6	166	*YES*
Mode 4D	5.0e7	*D < 20%*		*no*
Mode 1E	2.0e7	28.2	46	*YES*
Mode 2E	2.0e7	27.3	54	*YES*
Mode 3E	3.5e7	35.0	102	*YES*
Mode 4E	5.0e7	28.2	164	*YES*
Mode 5E	5.0e7	49.4	254	*no*
Mode 6E	5.0e7	52.1	332	*no*

Table 5. Required bearing damping $D_{20\%}$

From the comparison between both configurations it turns out that the configuration ‘E’ is more gentle than ‘D’ because

the shaft requires less damping input and thus less force to achieve a satisfying modal damping.
To generate the damping the transfer function must have gain and a phase lag within 0-180 degree. With increasing frequency it becomes more difficult to provide high damping coefficients: on one side, the damping coefficient is proportional the relation 1/ω, on the other side the bearing gain is limited by the amplifier low pass filter characteristics depending on current and voltage limitations as exemplary reported by Alban et al. (2009). The bearing coefficients are defined with the equations

$$C_{BRG} = G \cdot \cos\varphi \qquad (2)$$

G: Gain [N/m]
C_{BRG}: Bearing Stiffness [N/m]

$$D_{BRG} = G \cdot \sin\varphi / \omega \qquad (3)$$

φ: Phase [degree]
D_{BRG}: Bearing Damping [Ns/m]

Where G is the gain of the transfer function and φ is the corresponding phase.

Figure 19 shows the determined $D_{20\%}$ for the modes at or below the maximum continuous speed. The lines of constant gain used to damp the system (D_{BRG}, c.f. Equation 3) are plotted in light grey. Those impedance isolines demonstrate the difficulty to achieve a large damping coefficient at high frequency and are useful to evaluate the ability to damp the modes. Additionally the exemplary damping coefficient path of the transfer function discussed in the bearing characteristics chapter (Figure 13) is superimposed.
Even if modes 1D and 3D have approximately the same $D_{20\%}$ it is clear that mode 3D is the critical one for the machine and the control loop layout as the gain necessary to generate $D_{20\%}$ is nearly 5 time higher than the one of 1D. Mode 4E needs considerably less damping gain than mode 3D.

Modes 1E, 2E and 1D lie near the same impedance isoline (10'000 kN/m) and thus need similar damping effort even if the frequencies of the modes $NF_{20\%}$ are different. Comparing the modes and considering the exemplary bearing damping coefficient curve mode 1D has less margin than the other two. In the medium frequency range Mode 2D is easier to handle than mode 3E.

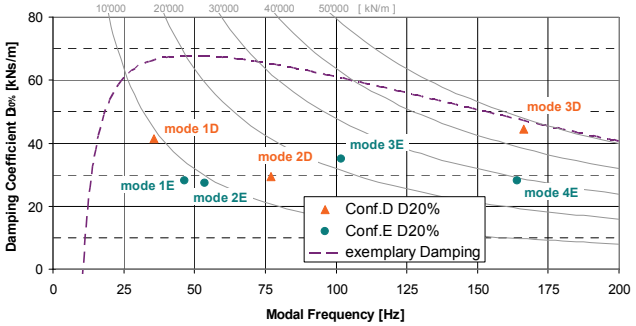

Figure 19. Required $D_{20\%}$ over frequency.

The bearing stiffness selected for the various modes in Table 5 are based on a typical controller layout. For a deeper comparison between configurations 'D' and 'E', the bearing stiffness is parameterized and varied from c_{BRG}=1e6 N/m up to 1e8 N/m in seven steps. Of course the bearing stiffness can easily be higher than this. As we analyze the behavior of $D_{20\%}$, going to beyond 100 MN/m is uninteresting as many modes cannot anymore be critically damped and therefore $D_{20\%}$ is not defined for them. Note that the modal damping of mode D1 doesn't reach the threshold of 20 percent from bearing stiffness c_{BRG} ~ 60MN/m upwards.

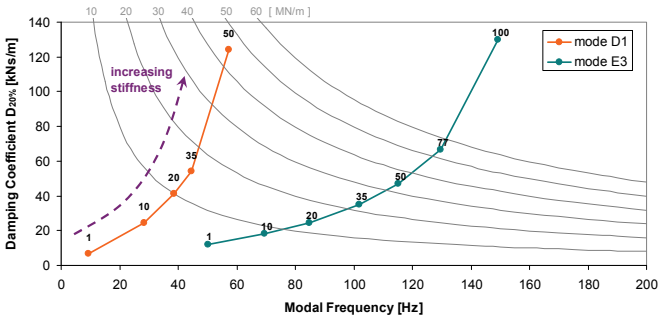

Figure 20, Required $D_{20\%}$ over frequency, with bearing stiffness c_{BRG} denoted in MN/m as parameter.

The results of the analysis are presented in Figure 20. The labels at the dots in the graph are the bearing stiffness c_{BRG} in MN/m, a unity selected to shorten the notation on the graph. This graph shows only mode D1 and E3 as they are the 1st bending modes relevant for the stability analysis. Mode E1 and E2 are rigid body modes (see Figure 12).
Typically modes need more damping at stiffer bearings. However there are differences in the sensitivity to that stiffness. Also the frequency dependency of the mode is clearly different. As confirmed by Figure 20 a low bearing stiffness is favorable for the damping effort. Unfortunately this is a major drawback as aerodynamic perturbations at the border of the performance map (e.g. near to surge conditions) can rapidly lead to high vibrations and therefore machine tripping. The vibration amplitudes induced by the disturbance are inversely proportional to the stiffness. Therefore a high stiffness at low frequency (as long as the AMB system is able to deliver it) is preferred. The consequence is that mode D1 doesn't allow much flexibility for the tradeoff between stiffness and damping, whereas mode E3 is gentler.
Another conclusion from the curves in Figure 20 is related more closely to the modal frequencies. The flexi ratio of the stability relevant mode E3 is constantly higher than the one of mode D1, leading to a more robust behavior.
The third comparison of those two modes focuses on the damping effort or damping gain. Up to a bearing stiffness of 35 MN/m (3.5e7 N/m) mode D1 requires less effort of the AMB system than mode E3. This becomes visible when the damping gain isolines are pursued. However at higher bearing stiffness mode D1 becomes difficult to damp and surpass mode E3 in the damping gain requirements.

Concluding from this analysis it can be stated that, thanks to the shaft rigidity, configuration 'E' is more robust as 'D'. The illustrated damping coefficient curve from the transfer function could be different, but the stated qualities, advantages and downsides are confirmed by the additional variation of the system bearing's stiffness.

TORSIONAL ANALYSIS

Critical Speeds

Compressor trains are subjected not only to lateral but also to torsional vibrations. Therefore a torsional analysis is performed for each configuration according to API 617 (2002). Hence the compressor and (if applicable) the Low-Speed trains are screen for potential torsional resonance problems.

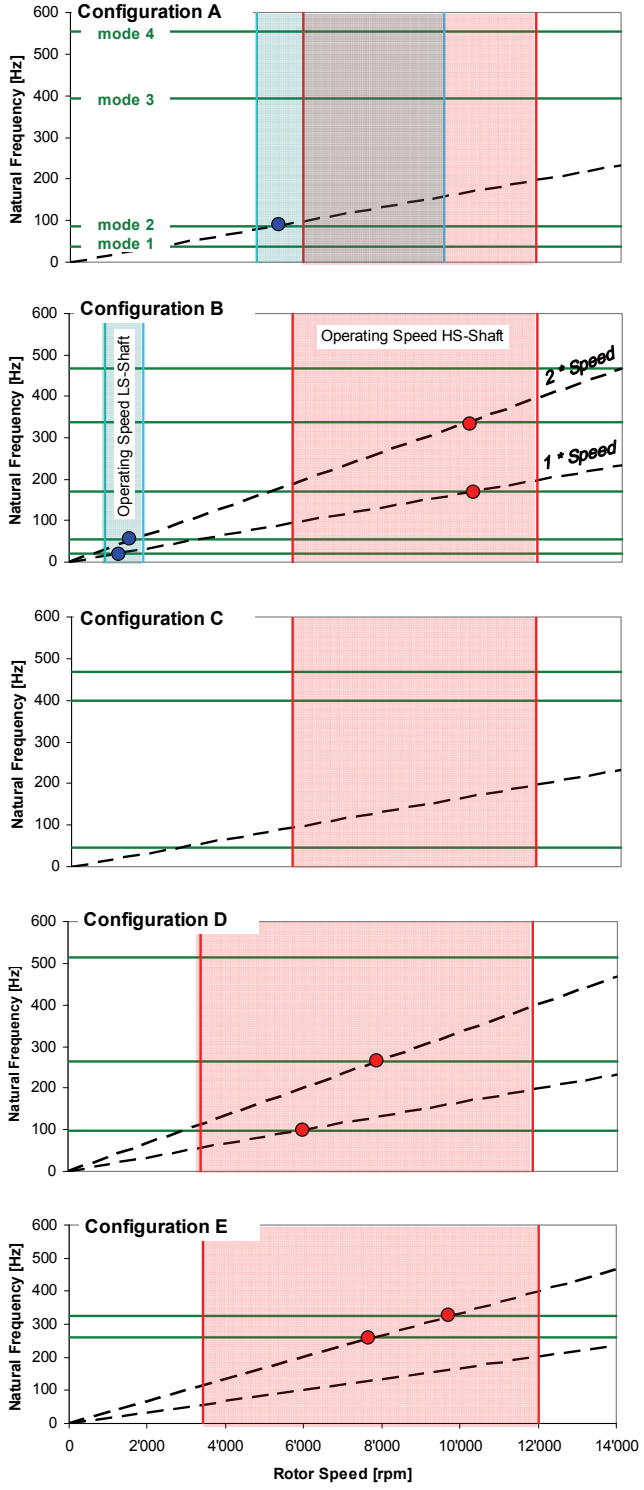

Figure 21: Torsional Campbell diagrams (mechanical)

Figure 21 shows the calculated undamped torsional natural frequencies in a Campbell diagram for each configuration. The horizontal green lines represent the torsional critical speeds. Due to the wide operating range it's impossible to avoid resonances provoked by excitations at 1x and 2x of rotational speed in most configurations. The resonances corresponding to any excitation due to 1x Speed and (for the motor driven configurations) to 2x Speed excitations are represented with a filled circle.

The comparison between the Campbell diagrams clearly shows the advantage of configuration 'C' (gas turbine driver without gear) because no resonance occurs. Generally from the results it can be stated that the motor driven configurations present more resonances than the gas driven units because of the consideration of the excitation due to 2x speed.

In terms of coincidences in the operation range the worst configuration is probably configuration 'A'. Together with a relatively small gear ratio the big speed range leads to a merge of the low and high speed prohibitive regions. In many cases it will not be possible to drag the eigenfrequencies out of the range. The bigger gear ratio of configuration 'B' provides a window between low speed speed range and high speed speed range where the resonance can be tuned in. But on the other side the 1x and 2x per revolution coincidences have to be considered.

Harmonic Response Analysis (mechanical)

The criticality of a mode depends both on the magnitude of excitation as well as on the train's mode shape. If the mode shape does not show any deflection at the source location the resonance can not build up and no stresses are induced in the shafts. If the converse happens the stresses induced depend linearly from the excitation magnitude. Due to this linearity the induced stresses of coinciding modes in the speed range have been calculated for the following load cases (if applicable):

- 1 percent rated torque at driver (abbreviated with DR)
- 1 percent rated torque at gearbox (abbreviated with GB)

Load case	Frequency	Calculated Stress	Calculated Moment
	[Hz]	[Nmm^{-2}]	[p.u.]
Configuration 'A'			
GB	87	17.1	0.36
Configuration 'B'			
DR	20	15.6	0.58
GB		5.7	0.21
DR	54	1.2	0.03
GB		9.6	0.20
DR	169	0.04	<0.01
GB		0.03	<0.01
DR	337	0.3	<0.01
GB		0.01	<0.01
Configuration 'C'			
-	*No coincidences*		
Configuration 'D'			
DR	98	6.4	0.25
DR	265	0.5	0.03
Configuration 'E'			
DR	260	0.7	0.05
DR	325	1.6	0.13

Table 6. Highest induced stresses and moments (mechanical).

For both load cases the highest stress occurring in the shaft system is tabulated in Table 6. As calculations are always done with 1 percent rated torque the results can be scaled by the maximum expected excitations. Additionally the torque responses to the normalized torque quantify the mode "excitability". It has to be noted that the highest torque and the highest stress in the shaft can be at different location. In the calculation of torque and stress the diameter of the shaft element plays a different role. The torque is scaled with the shaft rated torque in order to allow a comparison between shafts with different speeds.

Configuration 'A' has only one coincidence at 87 Hz. This frequency can be excited at the gearbox location only (the gas turbine driver has virtually no excitation at 1x and 2x speed). The induced stress is 17.1 N/mm2 and the normalized torque is 0.36 p.u. Configuration 'B' has a electrical motor driver and can therefore be excited both by the driver and the gearbox. A single coincidence results in two stress levels and force impacts. For this configuration the worst mode is at 20 Hz when the driver excites the system. The torsional modes at 169 Hz and 337 Hz lead to a negligible level of stress. The magnetically levitated configurations 'D' and 'E' are excited only at driver location (no gearbox). Arrangement 'D' has a coincidence with the 1x speed with a level of 0.25 p.u. whereas configuration 'E' has only coincidences with the 2x speed and a maximum excitability of 0.13 rated torque.

Regarding the excitability the best configuration besides 'C' (no coincidences) is train 'E'. Configuration 'A' is better than 'B' but worse than 'D'. The advantage of configuration 'A' over 'D' and 'E' is that it can not be excited by the driver and his harmonics air gap torques treated in the next chapter.

Harmonic Response Analysis (electrical

Additionally to the critical speeds provoked by the so-called mechanical excitations the electrical excitations must be considered for the trains driven by a motor and equipped with a frequency converter. Integer and non-integer harmonics are generated in the inverter. An excitation torque is transferred through the motor air gap into the motor rotor. The frequency of these excitations can lead to torsional resonances. In the literature measurements show high torque oscillating amplitude caused by high torques initiated by the inverter. Torque excitation can lead to catastrophic failure within the shaft system.

A more detailed explanation about the sources of excitations and impact on the compressor system has been presented by Hütten, et al. (2011) and Terens and Grgic (1996). The excitations of concern are split into two categories: the integer harmonic torque pulsation and the non-integer air gap torque pulsation. Whereas the frequency of the integer harmonics are simply proportional to the motor speed the frequency of the non-integer harmonics are a function of the line frequency, the motor speed and the pole number of the motor.

The magnitude of the exciting torques is influenced by several factors and can even be increased by a speed control feedback mechanism. Therefore the determination of the actual resulting resonance shear stress in the shaft is challenging. In many cases the only remaining solution is to experimentally determine the dynamic loading of the coupling by torque measurements.

Figure 22 shows a typical electrical Campbell diagram for configuration 'B' with integer (6fM) and non-integer (6|fN-fM|, 12|fN-fM| and |6fN-12fM|) harmonic excitation frequencies superimposed, where fN is the grid frequency and fM is the actual motor operating frequency.

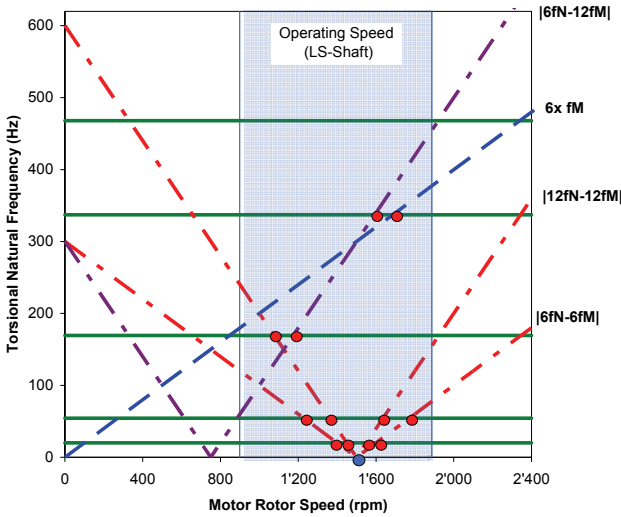

Figure 22. Torsional Campbell diagram (electrical, Conf. 'B').

This diagram shows many resonances within the operating range excited by the electrical harmonic frequencies. Especially the experience from several strain gauge measurements performed by the author's company reveals that the dynamic torques at the resonance corresponding to the 6|fN-fM| excitation at the first torsional natural frequency are not negligible. Thus it can be necessary to implement a small barred speed range around these critical speeds. However this means a limitation of the production flexibility.

Whereas the integer harmonic has to be considered only for trains with a low speed shaft (for high speed shaft the frequencies are to high by far), the non-integer harmonics are not only an issue for configuration 'B' but also for the magnetically levitated trains.

In contrast to the VFD configuration with gearbox the directly driven high speed motors have only one pole pair. The consequence is that the lines exemplary shown in Figure 22 have half their slope and the point on the bottom – blue dot denoted as PS - is not at 1500 rpm anymore but at 3000 rpm. The only natural frequencies that cannot have a coincidence with the non-integer harmonics are those below the crossing of 6|fN-fM| and the lower boundary of speed range. This crossing is calculated by inserting the minimum speed in the equation 6|fN-fM|. For configuration 'D' this is 37.5 Hz. It's clear that mode 1 (currently at 98.7 Hz) can not be tuned below that value and therefore there will always be a coincidence with this specific non-integer harmonic.

For configuration 'E' it is not even worth to calculate the maximum frequency. The directly coupled system doesn't offer that much tuning opportunities and coincidences with non-integer harmonics are present in any case.

Load case	Frequency	Calculated Stress	Calculated Moment
	[Hz]	[N/mm²]	[p.u.]
Configuration 'A'			
DR	*Gas turbine driven*		
Configuration 'B'			
DR	20	31.2	1.16
DR	54	2.4	0.05
DR	169	0.1	<0.01
DR	337	0.6	<0.01
Configuration 'C'			
-	*Gas turbine driven*		
Configuration 'D'			
DR	98.	12.8	0.50
DR	265	1.0	0.05
Configuration 'E'			
DR	260	1.4	0.10
DR	325	3.2	0.25

Table 7. Highest induced stresses and moments (electrical).

Because the stress level decays rapidly after the first two to three eigenfrequencies, coincidences higher than 350 Hz are not considered anymore. For the coincidence with a non-integer harmonic 2 percent of rated torque is considered as ripple content, regardless if a voltage source inverter (cleaner output) or a current source inverter (cheaper) is used.

The natural frequency of 20 Hz in configuration 'B' reacts with 31.2 N/mm2 to the air gap torque of the driver. Non-integer harmonics are calculated to induce 12.8 N/mm2 in the configuration 'D' and 3.2 N/mm2 for configuration 'E'. Between the stress levels of configuration 'B' and 'E' there is a factor of ten. The flexibly coupled configuration 'D' has exactly 4 times more stress level.

The best train is the direct gas turbine driven compressor in configuration 'C'. There are no coincidences and virtually no excitations. For the run up too, there is only one single critical torsional speed – where the coupling strains - , simplifying the barred speeds below minimal operation speed (50 percent).
Configuration 'D' and 'E' are similar. The difference is that 'D' has both coincidences with the 1x and 2x speed, while configuration 'E' has only coincidences with the 2x speed. The stress level of configuration 'D' is higher than in the last configuration. As active magnetic bearing machines are normally driven by voltage source inverters the 2 percent torque applied to the load case DR is very conservative (In most cases the ripple content of such inverters can be neglected).
Under the consideration of the torsional critical speeds and the corresponding stress levels a ranking of the configurations is performed:

- Conf. 'C' (no resonance)
- Conf. 'A' (one critical speed at LS-shaft)
- Conf. 'E' (two critical speeds due to 2x speed excitation)
- Conf. 'D' (two critical speeds, one at 1x speed excitation)
- Conf. 'B' (several critical speeds, due to mechanical and electrical excitations)

Also with regard to the torsional integrity configuration 'B' is more critical than configuration 'A'.

If the motor would be driven by a voltage source inverter, then configurations 'B', 'D' and 'E' would have a better rating in the torsional analysis.

CONCLUSION

The aim of the paper is to compare the five presented solutions for gas storage applications. Table 8 gives a qualitative overview for the five discussed configurations.

Configuration	'A'	'B'	'C'	'D'	'E'
Criteria					
Lateral Harmonic Response	+	+	+	o	-
Cpl. Unbalance Sensitivity	o	-	o	--	++
Level I Stability	-	-	-	+	++
Torsional	+	--	++	-	-
Ranking	**3**	**5**	**1**	**4**	**2**

Table 8. Overview of strength and weaknesses.

The direct gas turbine driven compressor – configuration 'C' – is good-natured regarding the train torsional behavior. The lateral analysis classifies this compressor between solutions 'A' and 'B' because of the coupling unbalance sensitivity. The stability behavior (basic LogDec δ_b and Q_0) is equal for the three configurations 'A', 'B' and 'C'. If a gas turbine drive is mandatory, configuration 'C' is the best in terms of simplicity, rotordynamics and footprint. Thanks to the fact that no gearbox is needed, even the efficiency increases (losses for a 7 MW gearbox are in the region of 150 kW, which is 2 percent).
Configuration 'B' has higher coupling unbalance sensitivity, has many torsional resonances, in particular the lowest mode (20 Hz) which is excited to a considerable stress level. Hence a torsional measurement is recommended, maybe leading to a small barred speed ranges. This configuration is clearly the most difficult to handle.
Configuration 'A' has neither the coupling sensitivity drawback nor the torsional complications as the driver is a gas turbine and is therefore rated as third best solution.

If the view can be extended to sealed, magnetically levitated systems, it is arguable that configuration 'C' is slightly better rated than 'E'. In this case the decision may be driven by other considerations, like auxiliary systems, gas turbine rotordynamics (contain risks too), ecological aspects and service requirements (e.g. ramp up times), which are not addressed by this paper. The main advantages of configuration 'E' are the better coupling sensitivity and the promising stability key figures. When comparing the two design with magnetic bearing technology 'D' and 'E' the last configuration has better damping qualities leading to less required damping effort to accomplish the amplification factor requirements and a better overall stability behavior. The advantages of configuration 'E' in the torsional analysis are negligible and thus the trains design considered coequal for this figure. On the other side, favorable arguments for configuration 'D' would be a smaller alignment effort at manufacturer workshop and less critically damped speeds in the speed range, both a direct profit from the flexible coupling.

Generally, due to its compactness, configuration 'E' probably requires more manufacturing attention than the other

compressor train arrangements. Indeed the controller design for a four bearing rotor is more complex than for a two bearing system however several running units of this type prove that the required knowhow is present in the Oil & Gas industry.

While the conventional trains are available from several manufacturers and in any power class, the magnetically levitated, direct driven concepts are limited to 20 MW and few suppliers of motor, VFD, compressors and magnetic bearings. The voltage source inverter technology is one of the main subjects where further developments are welcome to increase the available power at a given speed. As the gas market is nowadays driven by the notion of a relatively clean energy source the increasing demand is surely activating an evolution of the available high speed configurations by the supplier operating in these technologies and applications. In the future gas storage operators will be able to select compressors trains out of a broader machine spectrum with extended power capability.

NOMENCLATURE

AF	= Amplification Factor	[-]
C_{BRG}	= bearing stiffness	[N / m]
C_{eff}	= effective bearing stiffness	[N / m]
CSR	= Critical Speed Ratio on Rigid Supp.	[-]
D_{BRG}	= bearing damping	[Ns / m]
$D_{20\%}$	= bearing damping when mode-AF=2.5	[Ns / m]
$NF_{20\%}$	= mode frequency when mode-AF=2.5	[Hz]
f_{mode}	= Natural frequency	[Hz]
f_N	= grid frequency	[Hz]
f_M	= motor shaft frequency	[Hz]
G	= Gain of transfer function	[N/m]
$G_{req.}$	= Gain req. for mode AF=2.5	[N/m]
M_{CH}	= half coupling mass	[kg]
N_{mcs}	= max. continuous speed	[rpm]
U_{Cpl}	= Coupling Unbalance	[gmm]
φ	= Phase of transfer function	[degree]
$\varphi_{req.}$	= Phase lag req. for mode AF = 2.5	[degree]
ω	= rotor angular velocity	[rad / s]
δ_b	= basic logarithmic decrement	[-]
δ_A	= logarithmic decrement with Q_A	[-]
Q_A	= Anticipated Cross Coupling	[kN/mm]
Q_0	= Cross coupling when LogDec = 0	[kN/mm]
$SM_{req.}$	= required separation margin	[-]
$SM_{effect.}$	= effective separation margin	[-]

REFERENCES

Alban T. and al., 2009, “Mechanical and performance testing method of an integrated high-speed motor compressor”, Proc of. 38th Turbomachinery Symposium, Turbomachinery Laboratory, Departement of Mechanical Engineering, Texas A&M University, College Station, Texas, USA.

API 617, 2002, “Axial and Centrifugal Compressors and Expander-compressors for Petroleum, Chemical and Gas Industry Services”, Seventh Edition, American Petroleum Institute, Washington, D.C.

API 671, 2007, “Special Purpose Couplings for Petroleum, Chemical and Gas Industry Services”, Fourth Edition, American Petroleum Institute, Washington, D.C.

Hütten, A. and al., 2011, “VSDS Motor Inverter Design Concept for Compressor Trains avoiding Interharmonics in Operating Speed Range”, Proc. of the First Middle East Turbomachinery Symposium, Doha, Qatar.

Kleynhans G., and al., 2005, “Hermetically Sealed Oil-Free Turbocompressor Technology”, Proc of. 34th Turbomachinery Symposium, Turbomachinery Laboratory, Departement of Mechanical Engineering, Texas A&M University, College Station, Texas, USA.

Terens, L and Grgic, A., 1996, “Applying Variable Speed Drives With Static Frequency Converters to Turbomachinery”, Proc. Of 25th Turbomachinery Symposium, Turbomachinery Laboratory, Departement of Mechanical Engineering, Texas A&M University, College Station, Texas, USA.